Available online at www.sciencedirect.com
SCIENCE DIRECT®
ELSEVIER
Applied Numerical Mathematics 56 (2006) 1271–1282
APPLIED NUMERICAL MATHEMATICS
www.elsevier.com/locate/apnum

On the finite element method on quadrilateral meshes

Daniele Boffi

Dipartimento di Matematica "F. Casorati", Pavia, Italy

Available online 16 May 2006

Abstract

The theoretical analysis of the finite element method is well established in the case of triangular or tetrahedral meshes. In this case optimal approximation properties have been proved in all reasonable functional norms. Several commercial codes use this method which is now in the common practice of engineering applications. On the other hand, the case of quadrilateral or hexahedral meshes, even if commonly used in the applications (sometimes it seems to be even more popular than the previous one), has not been studied in such deep detail, probably because it hides some insidious issues. For simplicity, we restrict our analysis to the two-dimensional case; three-dimensional analysis in some cases is a straightforward extension, in some others is more complicated. Indeed, we shall show that some commonly used quadrilateral finite elements present a lack of convergence when general regular meshes are used. The list of suboptimal elements includes serendipity (or trunk) elements, face elements, edge elements. A rigorous theory is presented, which gives necessary and sufficient conditions for optimal order approximation. Our theory is supported by several numerical experiments, which are taken from various engineering applications, ranging from elasticity and fluid dynamics to acoustics and electromagnetics. Example of suboptimal elements include: 8-node element for Poisson problem, Q_2–P_1 Stokes element, face elements for acoustic problem, edge elements for electromagnetic problems.

MSC: 65N30; 41A10; 41A25

Keywords: Quadrilateral; Finite elements; Approximation; Serendipity; Mixed finite elements

1. Introduction

In this paper we review in a unified approach results concerning the approximation properties of quadrilateral finite elements on general regular (possibly nonaffine) meshes. These results have been presented recently to the mathematical community; the main references are [2] for the scalar case, [7] for the Stokes problem, [1] for several numerical tests, [4] for the vector case, and [3] for possible consequences for the Reissner–Mindlin plate. We believe that these results are of great importance for the design of quadrilateral finite elements and the aim of this contribution is to provide the mathematical and engineering community with a unified analysis of this topic. Some new numerical results are presented for the first time in Section 8. This paper contains results which generalize the classical finite element theory presented, for instance, in [12,13], and which improve the approximation theory for quadrilateral vector valued finite elements presented in [17].

In this section we give a detailed description of the structure of the paper and we introduce the main results.

E-mail address: daniele.boffi@unipv.it (D. Boffi).
URL: http://www-dimat.unipv.it/boffi/.

doi:10.1016/j.apnum.2006.03.027

In Section 2 we recall the definition of quadrilateral finite elements with particular emphasis on the transformations from the reference (master) element to the actual (physical) one. We shall distinguish between the cases of scalar and vector functions. Indeed, in the former case, we consider the standard mapping (based on the pull-back) which preserves the function continuity. For the latter case, we shall handle two different situations. On one side, if we are interested in the continuity of the normal component (like in problems arising from elasticity or acoustics, when the underlying functional space is $H(\mathrm{div};\Omega)$), we shell consider the Piola (contravariant) transform. On the other side, when the continuity of the tangential component is of interest (as it is the case for problems arising from electromagnetism which involve the space $H(\mathrm{curl};\Omega)$), we shall consider the covariant transform.

In Section 3 we study in detail the scalar case. We are interested in optimal approximation estimates for the function and its gradient in the $L^2(\Omega)$ norm, which read

$$\inf_{v\in V_h}\|u-v\|_{L^2}=\mathrm{O}\big(h^{k+1}\big), \tag{1}$$

$$\inf_{v\in V_h}\big\|\mathrm{grad}(u-v)\big\|_{L^2}=\mathrm{O}\big(h^{k}\big) \tag{2}$$

where h refers, as usual, to the mesh parameter and the finite element space V_h contains polynomials of degree k. The main result of this section is that estimates (1), (2) hold on general regular quadrilateral meshes if and only if the reference finite element space contains $\mathcal{Q}_k$, the space of polynomials of degree at most k in each variable, separately.

In Section 4 we extend the theory presented in Section 3 to the case of vector-valued functions. Since in the 2D case the space $H(\mathrm{div};\Omega)$ and $H(\mathrm{curl};\Omega)$ are isomorphic (a rotation of $\pi/2$ maps the divergence operator to the curl one), we shall only describe the $H(\mathrm{div};\Omega)$ case. The extension to the vector case is not a straightforward application to the results of the previous section. We are interested in optimal approximation estimates of the vectorfields and their divergences in the $L^2(\Omega)$ norm; namely

$$\inf_{\mathbf{v}\in V_h}\|\mathbf{u}-\mathbf{v}\|_{L^2}=\mathrm{O}\big(h^{k+1}\big), \tag{3}$$

$$\inf_{\mathbf{v}\in V_h}\big\|\mathrm{div}(\mathbf{u}-\mathbf{v})\big\|_{L^2}=\mathrm{O}\big(h^{k+1}\big). \tag{4}$$

Also in this case, we shall show necessary and sufficient conditions for estimates (3), (4) to hold, which characterize the finite element space on the reference element. Such conditions are a little more complicated to describe than the previous one and we do not anticipate them in this introduction.

In Section 5 we present a first application of the results concerning the scalar case. We consider the approximation of the Laplace/Poisson problem on a square and demonstrate numerically that our theoretical results presented in Section 3 are sharp. In particular, we show that commonly used serendipity (or trunk) elements on general quadrilateral meshes present a lack of convergence. This is the case for the 8-node element which is asymptotically second order accurate in $L^2(\Omega)$ as compared to the full 9-node element which presents a third order behavior.

In Section 6 we present the application of the results of Section 3 to the popular Q_2–P_1 Stokes element. We shall recall that two approaches are possible in order to define the pressure space. A local approach (where the functions are mapped as described in Section 2) and a global approach (where the pressures are not mapped from the reference element to the actual one but are linear functions defined on the physical element). We recall that the classical inf-sup stability condition is satisfied for both approaches, but, according to the results of Section 3, the local approach cannot provide optimal order of convergence, since the reference pressure space does not contain all of $\mathcal{Q}_1$. For this reason, on general quadrilateral meshes, the global approach is to be preferred. Numerical tests confirm the bad behavior of the local approach; it is interesting to notice that, as it should be expected when dealing with mixed methods, the suboptimal convergence of the pressures implies a bad convergence of the velocities as well.

In Section 7 we consider a first application of the results presented in Section 4 concerning the approximation of vector-valued functions. Several numerical results confirm our theory, showing, in particular, that the popular Raviart–Thomas element does not achieve optimal convergence on general quadrilateral meshes. A new mixed finite element family introduced in [4] proves to be optimal order convergent also on highly distorted meshes.

In Section 8 we consider the application of the results presented in Section 4 to two eigenvalue problems. Again, using the isomorphism between the divergence and the curl operator in two space dimensions, we restrict our analysis to the case of $H(\mathrm{div};\Omega)$ approximation and to the eigenvalue problem arising from acoustics. Numerical experiments confirm the theory and show that the lowest order Raviart–Thomas element provide stable, but *not convergent* solutions on distorted meshes. Some new numerical results show that higher order Raviart–Thomas elements provide suboptimally convergent solutions. On the other hand, the new family of finite elements introduced in [4] presents optimal convergence behavior.

2. Quadrilateral finite elements

We denote by $\widehat{K}$ the unit reference square and by K a generic quadrilateral element of a triangulation $\mathcal{T}_h$ of Ω. For simplicity, we assume that Ω is a two-dimensional polygonal domain and that the mesh matches exactly with Ω, so that we do not have to care about the approximation of the boundary of Ω. The mapping $F_K : \widehat{K} \to K$ is a bilinear function (it is not uniquely defined; we suppose to pick up a particular choice). If F_K is affine then K is a parallelogram and conversely.

We shall make use of *regular* mesh sequences; there are different possibility on how to measure the shape regularity of a mesh. One possible choice is the following one. From the quadrilateral K we obtain four triangles by the four possible choices of three vertices from the vertices of K, and we define ρ_K as the smallest diameter of the inscribed circles to these four triangles. The *shape constant* of K is then $\sigma_K := h_K/\rho_K$ where $h_K = \operatorname{diam}(K)$. A bound on σ_K implies a bound on the ratio of any two sides of K and also a bound away from 0 and π for its angles (and conversely such bounds imply an upper bound on σ_K). It also implies bounds on the Lipschitz constant of $h_K^{-1} F_K$ and its inverse. The shape constant of a mesh consisting of convex quadrilaterals is then defined to be the supremum of the shape constants σ_K for all K, and a family of such meshes is called shape-regular if the shape constants for the meshes can be uniformly bounded.

A finite element space of *scalar* functions is usually defined by means of a finite dimensional space $\widehat{V}$ (typically made of polynomials) of functions on the reference element $\widehat{K}$. On the actual element K, the finite element space can be defined by means of the pull-back operator (composition with the inverse of F_K) as follows

$$V_F(K) = \left\{ v : K \to \mathbb{R}:\ v = \hat{v} \circ F_K^{-1} \text{ for some } \hat{v} \in \widehat{V} \right\}.$$

It should be noticed that $V_F(K)$ may contain nonpolynomial functions even if $\widehat{V}$ is a polynomial space. Indeed, in general, F_K^{-1} is not a polynomial unless F_K is affine. This is one of the major differences between triangular and quadrilateral elements.

This definition is a natural one and, by locating suitable degrees of freedom on the boundary of K, allows to enforce the continuity of functions across the elements.

When dealing with *vector-valued* finite elements, in several cases the continuity of the functions have to be understood component by component (this is the case, for instance when considering the velocity field in the approximation of fluid flows). If this is the case, we can just transform each component of the field as a scalar functions. In some other cases, however, only a weaker continuity is required. This is the case, for instance, when dealing with mixed approximation of Laplace equation where the flux variable is naturally in the functional space $H(\operatorname{div}; \Omega)$ consisting of fields in $L^2(\Omega)$ (square integrable fields) with divergence in $L^2(\Omega)$. Finite elements in $H(\operatorname{div}; \Omega)$ have normal component continuous across the elements, but the tangential component may in general be discontinuous.

In order to deal with functions in $H(\operatorname{div}; \Omega)$, we can consider the Piola (contravariant) transformation. Namely, given a function $\hat{\mathbf{v}} : \widehat{K} \to \mathbb{R}^2$, we define $\mathbf{v} = \mathbf{P}_F \hat{\mathbf{v}} : K \to \mathbb{R}^2$ by

$$\mathbf{v}\big(F(\hat{\mathbf{x}})\big) = JF(\hat{x})^{-1} DF(\hat{x}) \hat{\mathbf{v}}(\hat{x}),$$

where $DF(\hat{x})$ is the Jacobian matrix of the mapping F and $JF(\hat{x})$ its determinant. Given a reference finite dimensional space $\widehat{\mathbf{V}}$ of functions (typically polynomials in each component) defined on $\widehat{K}$, the finite element space $\mathbf{V}_F(K)$ on the actual element K is then defined as

$$\mathbf{V}_F(K) = \left\{ \mathbf{v} : K \to \mathbb{R}:\ \mathbf{v} = \mathbf{P}_F \hat{\mathbf{v}} \text{ for some } \hat{\mathbf{v}} \in \widehat{\mathbf{V}} \right\}.$$

When dealing with the space $H(\operatorname{curl}; \Omega)$ (vectorfields in $L^2(\Omega)$ with curl in $L^2(\Omega)$; this is the typical space used for modeling electromagnetic problems), the following covariant transformation can be used

$$\mathbf{v}\big(F(\hat{\mathbf{x}})\big) = DF(\hat{x})^{-T} \hat{\mathbf{v}}(\hat{x}),$$

which guarantees the continuity of the tangential component of the vectorfields across the elements (the normal component might be discontinuous).

The above mappings are natural in the sense that, by locating suitable degrees of freedom on the boundary of K, allow to enforce the continuity of the normal (tangential, respectively) component across the elements.

We explicitly observe that, since the operators div and curl are isomorphic in two space dimensions, the cases of $H(\mathrm{div};\Omega)$ and $H(\mathrm{curl};\Omega)$ can be handled simultaneously. For this reason, we shall restrict our analysis to the approximation theory of $H(\mathrm{div};\Omega)$.

3. Approximation properties of quadrilateral finite elements: the scalar case

The main result in this section is based on the following lemma (see [2]) that describes approximation properties on *rectangular* meshes. Here Ω is the unit square, decomposed into subsquares of size h, $\widehat{V}$ denotes the reference finite element on the reference square $\widehat{K}$, and V_h is defined as

$$V_h = \{u : \Omega \to \mathbb{R}\colon\ u|_K \in V_F(K) \text{ for all } K\}.$$

Lemma 1. *Let $\widehat{V}$ be a finite dimensional subspace of $L^2(\widehat{K})$, k a nonnegative integer. The following conditions are equivalent*:

(1) *there is a constant C such that* $\inf_{v\in V_h}\|u-v\|_{L^2(\Omega)} \leqslant Ch^{k+1}|u|_{k+1}$ *for all $u \in H^{k+1}(\Omega)$*;
(2) $\inf_{v\in V_h}\|u-v\|_{L^2(\Omega)} = \mathrm{o}(h^k)$ *for all polynomials u of degree at most k*;
(3) *$\widehat{V}$ contains all polynomials of degree at most k.*

We also need the following lemma (see again [2]).

Lemma 2. *The space $V_F(K)$ contains all polynomials of degree at most k for any quadrilateral K if and only if $\widehat{V}$ contains all polynomials of degree at most k in each variable, separately.*

By using a standard notation, we denote by $\mathcal{Q}_k$ the space of polynomials of degree at most k in each variable. The main result of this section consists in showing that the optimal approximation properties of order k on general quadrilateral meshes hold true *if and only if* $\widehat{V}$ contains $\mathcal{Q}_k$.

In order to get this result, we consider the mesh sequence described in Fig. 1. At each level, the mesh is obtained by translating and dilating a square macroelement made of four trapezoids.

Putting together Lemmas 1 and 2, and considering the mesh described in Fig. 1 we can state the main theorem of this section.

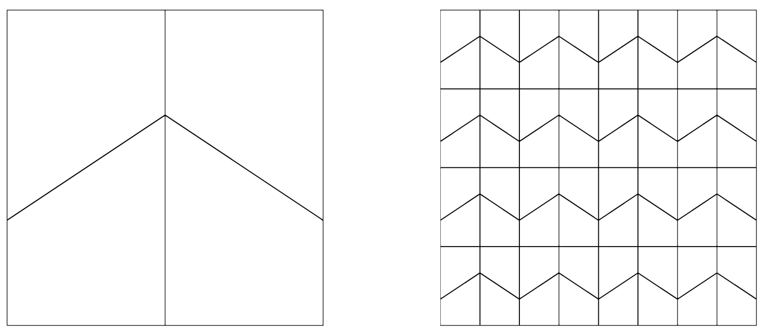

Fig. 1. The reference macroelement and a 4 by 4 mesh.

Theorem 1. *A finite element space sequence V_h associated to any mesh sequence of regular quadrilaterals provides optimal approximation estimates in $L^2(\Omega)$*

$$\inf_{v\in V_h} \|u - v\|_{L^2} \leqslant Ch^{k+1}|u|_{H^{k+1}} \tag{5}$$

if and only if $\widehat{V}$ contains $\mathcal{Q}_k$.

Proof. The sufficient part of the proof is a known result (see, for instance, [12]). The other implication follows from Lemmas 1 and 2 as follows. We present a mesh sequence such that the optimal estimate (5) does not hold true when $\widehat{V}$ does not contain $\mathcal{Q}_k$. In order to apply Lemma 1, let Ω be the unit square and consider the mesh sequence described in Fig. 1. The *rectangular* mesh of Lemma 1 is now the *macroelement* mesh of Fig. 1. It follows that, in order for Eq. (5) to hold, the finite element space V_h must contain all polynomials of degree at most k on each macroelement. From the result of Lemma 2, this is only possible if $\widehat{V}$ contains $\mathcal{Q}_k$. □

An analogous result for the approximation in the $H^1(\Omega)$ norm holds true (see [2]).

Theorem 2. *A finite element space sequence V_h associated to any mesh sequence of regular quadrilaterals provides optimal approximation estimates in $H^1(\Omega)$*

$$\inf_{v\in V_h} \left\|\mathrm{grad}(u - v)\right\|_{L^2} \leqslant Ch^{k}|u|_{H^{k+1}} \tag{6}$$

if and only if $\widehat{V}$ contains $\mathcal{Q}_k$.

The main consequence of the above theorems is that some commonly used finite element spaces do not provide optimal approximation on general regular quadrilateral meshes. We shall encounter some examples in Section 5 (8-node serendipity element) and 6 (unmapped local piecewise linears).

4. Approximation properties of quadrilateral finite elements: the vector case

In this section we extend the results of the previous one to the approximation in the $H(\mathrm{div};\Omega)$ norm when the finite element space is constructed by means of the Piola transform. As observed, in Section 2, similar results hold for the approximation in the $H(\mathrm{curl};\Omega)$ norm when the covariant transform is used in order to define the finite element space. We distinguish between the approximation in the $L^2(\Omega)$ norm and the approximation of the divergence in the $L^2(\Omega)$ norm and characterize the reference finite element spaces $\widehat{\mathbf{V}}$ which provide optimal estimates in the two cases. For simplicity, we only state the final results (the structure of the proof is similar to the one proposed in the previous section, but the arguments are not so immediate to describe).

In order to state our results, we recall some basic finite element spaces for the approximation of $H(\mathrm{div};\Omega)$. For a review of these spaces, we refer, for instance, to [11]. The Raviart–Thomas space $\mathbf{RT}_k$ is defined on the reference element as $\mathcal{P}_{k+1,k} \times \mathcal{P}_{k,k+1}$, where $\mathcal{P}_{i,j}$ denotes the space of polynomials of degree at most i in $\hat{x}$ and at most j in $\hat{y}$. We define the space $\mathbf{S}_k$ on the reference element as the subspace of $\mathbf{RT}_k$ of codimension one, where the vectors $(\hat{x}^{k+1}\hat{y}^k, 0)$ and $(0, \hat{x}^k\hat{y}^{k+1})$ are replaced by their combination $(\hat{x}^{k+1}\hat{y}^k, -\hat{x}^k\hat{y}^{k+1})$. We shall also make use of the space of scalar functions R_k defined on the reference element as the subspace of codimension one of $\mathcal{Q}_{k+1}$ where the term $\hat{x}^{k+1}\hat{y}^{k+1}$ is omitted.

The main results are stated in the following two theorems.

Theorem 3. *A finite element space sequence $\mathbf{V}_h$ associated to any mesh sequence of regular quadrilaterals provides optimal approximation estimates in $L^2(\Omega)$*

$$\inf_{\mathbf{v}\in \mathbf{V}_h} \|\mathbf{u} - \mathbf{v}\|_{L^2} \leqslant Ch^{k+1}|\mathbf{u}|_{H^{k+1}} \tag{7}$$

if and only if $\widehat{\mathbf{V}}$ contains $\mathbf{S}_k$.

Theorem 4. *A finite element space sequence* $\mathbf{V}_h$ *associated to any mesh sequence of regular quadrilaterals provides optimal approximation estimates of the divergence in* $L^2(\Omega)$

$$\inf_{\mathbf{v}\in\mathbf{V}_h}\left\|\operatorname{div}(\mathbf{u}-\mathbf{v})\right\|_{L^2}\leqslant Ch^{k+1}\left|\operatorname{div}(\mathbf{u})\right|_{H^{k+1}} \tag{8}$$

if and only if $\operatorname{div}\widehat{\mathbf{V}}$ *contains* R_k.

The main consequence of the above theorems is that all commonly used finite element spaces do not provide optimal approximation on general regular quadrilateral meshes. This is the case of $\mathbf{RT}_k$ element, since on the reference element it contains S_k (which implies optimal convergence in $L^2(\Omega)$) but $\operatorname{div}(\mathbf{RT}_k)$ does not contain R_k (which implies poor approximation of the divergence). The situation for other mixed spaces like $\mathbf{BDM}_k$ or $\mathbf{BDFM}_k$ (see [11]) is even worse, since they are suboptimal also in $L^2(\Omega)$ (see [4]).

For this reason, in [4] a new family $\mathbf{ABF}_k$ of mixed finite elements has been introduced such that $\mathbf{ABF}_k$ contains S_k and $\operatorname{div}(\mathbf{ABF}_k)$ contains R_k (which implies optimal approximation in $H(\operatorname{div};\Omega)$). On the reference element, we have $\mathbf{ABF}_k=\mathcal{P}_{k+2,k}\times\mathcal{P}_{k,k+2}$. With respect to $\mathbf{RT}_k$ the $\mathbf{ABF}_k$ space is obtained with the addition of some internal degrees of freedom (two bubbles when $k=0$).

5. Applications: Laplace problem

In this section we consider the standard finite element approximation of Laplace–Poisson problem: find $u:\Omega\to\mathbb{R}$ such that

$$\begin{aligned}-\Delta u&=f\quad \text{in }\Omega,\\ u&=g\quad \text{on }\partial\Omega.\end{aligned}$$

Here Ω is the unit square. We choose the data f and g such that the exact solution is the polynomial $u(x,y)=x^3+5y^2-10y^3+y^4$, so that no regularity issue is present.

In order to approximate the problem under consideration, we use the standard weak form involving the functional space $H^1(\Omega)$ and its finite element approximation: given $V_h\subset H^1(\Omega)$, find $u_h\in V_h$ with the prescribed boundary conditions such that

$$\int_\Omega \operatorname{grad}u_h\cdot\operatorname{grad}v=\int_\Omega fv\quad \forall v\in V_h\cap H_0^1(\Omega).$$

We consider the three mesh sequences plotted in Fig. 2: the first one is a uniform decomposition of Ω into subsquares, the third one is based on the macroelements shown in Fig. 1 and the second one (which we term *asymptotically*

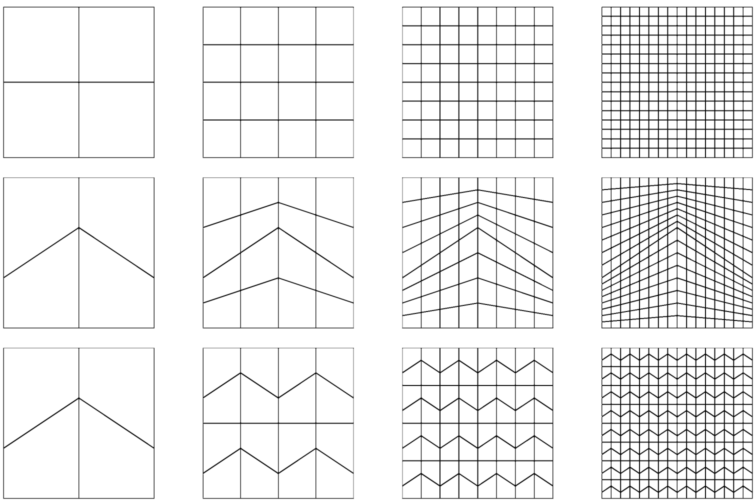

Fig. 2. Our mesh sequences.

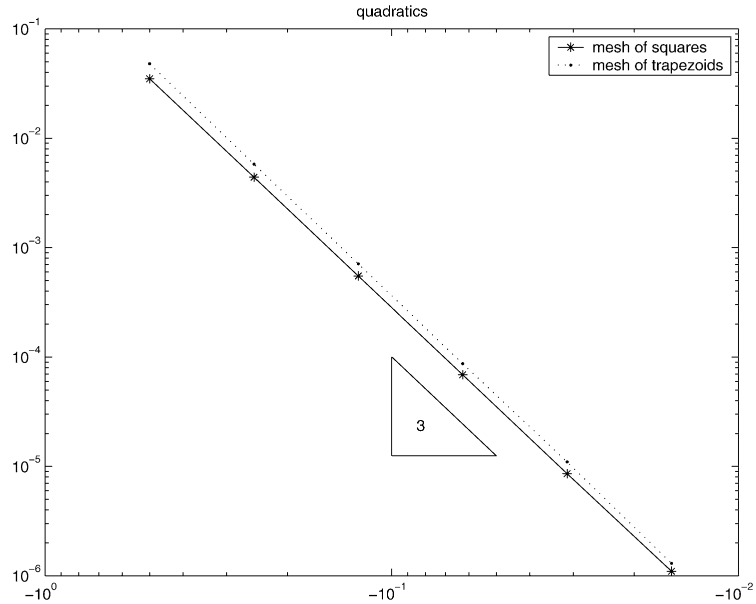

Fig. 3. Biquadratic approximation of Laplace equation.

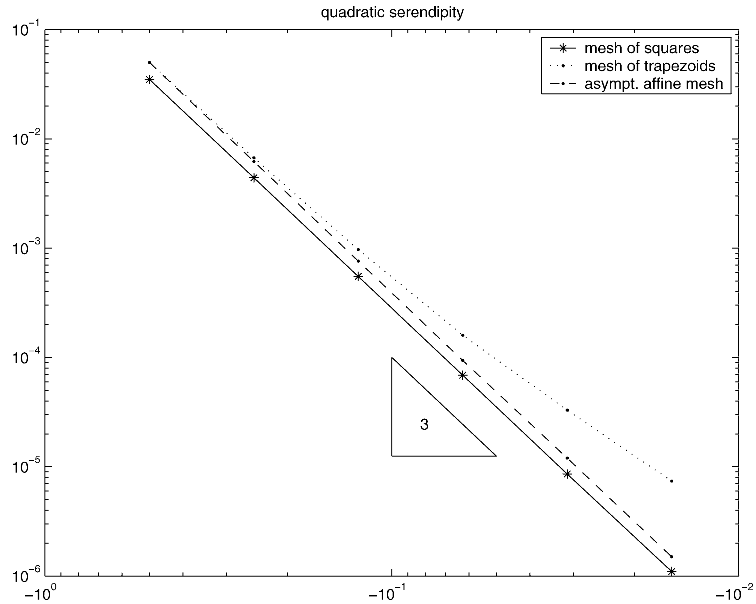

Fig. 4. Serendipity approximation of Laplace equation.

affine) is somewhat intermediate between the other two. It is clear that the first mesh should not give any trouble, while the third mesh is the one we used in Section 3 for our theory and will give rise to suboptimal results with certain choices of finite element spaces.

In Fig. 3 we report on the convergence history in the $L^2(\Omega)$ norm when standard 9-node biquadratic elements are used on the uniform mesh and the distorted one. It is apparent that the expected third order of convergence is achieved on both meshes.

On the other hand, the serendipity 8-node element, as shown in Fig. 4, is suboptimal on the distorted mesh. This is a crucial result which fully confirms our theory. On the other hand, the results on the asymptotically affine mesh are satisfactory (a proof of this result can be found in [2]).

6. Applications: Stokes problem

In this section we consider mixed finite element approximation of the Stokes problem: find $\mathbf{u} : \Omega \to \mathbb{R}$ and $p : \Omega \to \mathbb{R}$ such that

$$\begin{aligned} -\Delta \mathbf{u} + \operatorname{grad} p = \mathbf{f} &\quad \text{in } \Omega \\ \operatorname{div} \mathbf{u} = 0 &\quad \text{in } \Omega \\ \mathbf{u} = 0 &\quad \text{on } \partial\Omega. \end{aligned}$$

In order to approximate the problem under consideration, we use the standard mixed variational formulation which involves the space $H^1(\Omega)$ for the velocities and $L^2(\Omega)$ for the pressures. Given $V_h \subset H^1(\Omega)^2$ and $Q_h \subset L^2_0(\Omega)$, the approximate Stokes problem reads: find $\mathbf{u}_h \in V_h$ and $p_h \in Q_h$ such that

$$\begin{aligned} (\operatorname{grad} \mathbf{u}_h, \operatorname{grad} \mathbf{v}) - (\operatorname{div} \mathbf{v}, p_h) = (\mathbf{f}, \mathbf{v}) &\quad \forall \mathbf{v} \in V_h, \\ (\operatorname{div} \mathbf{u}_h, q) = 0 &\quad \forall q \in Q_h. \end{aligned}$$

It is well known that if the inf–sup condition

$$\inf_{q \in Q_h} \sup_{\mathbf{v} \in V_h} \frac{(\operatorname{div} \mathbf{v}, q)}{\|\mathbf{v}\|_{H^1} \|q\|_{L^2}} \geqslant \beta > 0$$

holds true, then we have the quasi-optimal error estimate

$$\|\mathbf{u} - \mathbf{u}_h\|_{H^1} + \|p - p_h\|_{L^2} \leqslant C \inf_{\mathbf{v} \in V_h,\, q \in Q_h} \big(\|\mathbf{u} - \mathbf{v}\|_{H^1} + \|p - q\|_{L^2}\big).$$

We shall consider the popular Q_2–P_1 element; namely, the velocities are approximated componentwise by continuous biquadratic elements and the pressures are discretized by discontinuous piecewise linears. Since the pressure need not be continuous, there are two natural ways of building the space Q_h: the first one consists in following the strategy presented in Section 2 and to consider a *local* (or mapped) approach (i.e., the pressures are mapped from the reference element to the physical one), while the second one considers a *global* (or unmapped) approach (i.e., the pressures are true linear functions defined directly on the physical element). If (ξ, η) denote the curvilinear variables on the element K and (x, y) the standard coordinates, then local pressures will be spanned by $(1, \xi$, and $\eta)$, while global pressures by $(1, x$, and $y)$.

From the theory presented in Section 3, it turns out that the correct choice should be to consider the global approach. Indeed, if the pressures are mapped from the reference to the actual element, then the reference space $\widehat{V}$ should contain all $\mathcal{Q}_1$ in order to provide optimal approximation order (and this is not the case, since it only contains linear functions).

Our numerical results confirm the theory, showing that the pressures are suboptimally approximated when the local approach is used on distorted meshes; see Fig. 5. What is not surprising (it is not predicted by our theory but is a reasonable behavior according to mixed methods), is that also the velocities are not optimally approximated when the local approach is used. This is demonstrated in the results shown in Fig. 6, where the $L^2(\Omega)$ velocity error is plotted.

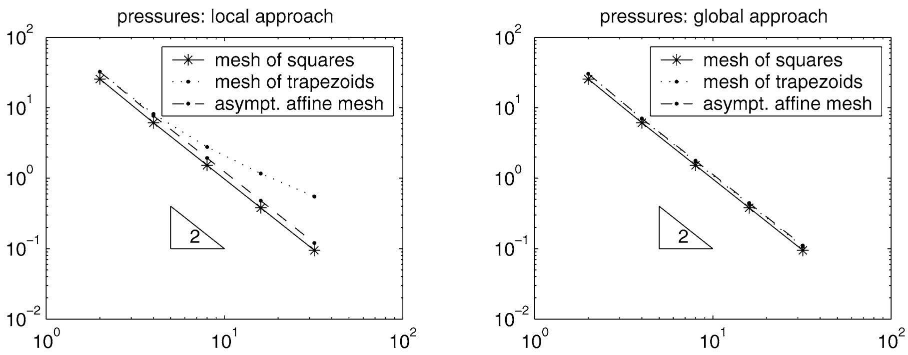

Fig. 5. Pressure approximation with the local (left) and global (right) approach.

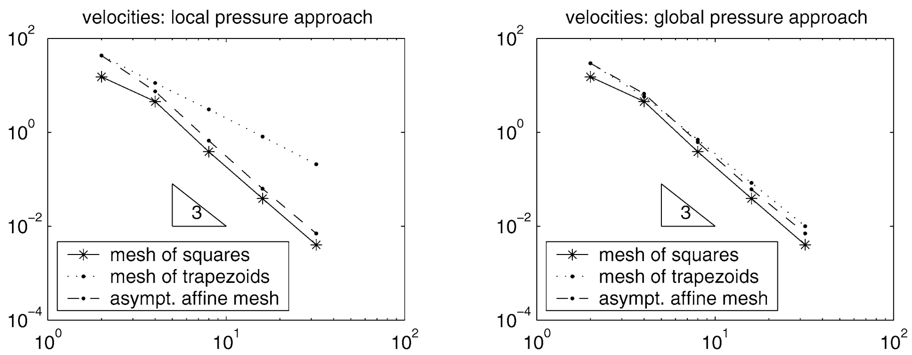

Fig. 6. Velocity approximation with the local (left) and global (right) approach.

Table 1
Errors and orders of convergence for the mixed approximation to Poisson's equation

$\mathbf{RT}_0$ on square meshes

n	$\|u-u_h\|_{L^2(\Omega)}$			$\|\boldsymbol{\sigma}-\boldsymbol{\sigma}_h\|_{L^2(\Omega)}$			$\|\operatorname{div}(\boldsymbol{\sigma}-\boldsymbol{\sigma}_h)\|_{L^2(\Omega)}$		
	err.	%	order	err.	%	order	err.	%	order
2	1.84e–02	55.28		6.09e–02	40.83		2.11e–01	30.15	
4	1.04e–02	31.07	0.8	3.32e–02	22.24	0.9	1.15e–01	16.43	0.9
8	5.33e–03	15.99	1.0	1.69e–02	11.34	1.0	5.86e–02	8.38	1.0
16	2.68e–03	8.05	1.0	8.49e–03	5.70	1.0	2.94e–02	4.21	1.0
32	1.34e–03	4.03	1.0	4.25e–03	2.85	1.0	1.47e–02	2.11	1.0

$\mathbf{RT}_0$ on trapezoidal meshes

n	$\|u-u_h\|_{L^2(\Omega)}$			$\|\boldsymbol{\sigma}-\boldsymbol{\sigma}_h\|_{L^2(\Omega)}$			$\|\operatorname{div}(\boldsymbol{\sigma}-\boldsymbol{\sigma}_h)\|_{L^2(\Omega)}$		
	err.	%	order	err.	%	order	err.	%	order
2	1.84e–02	55.08		6.34e–02	42.55		2.67e–01	38.14	
4	1.08e–02	32.37	0.8	3.63e–02	24.38	0.8	1.85e–01	26.51	0.5
8	5.60e–03	16.80	0.9	1.91e–02	12.83	0.9	1.53e–01	21.82	0.3
16	2.83e–03	8.48	1.0	9.81e–03	6.58	1.0	1.43e–01	20.42	0.1
32	1.42e–03	4.25	1.0	4.97e–03	3.33	1.0	1.40e–01	20.05	0.0

7. Applications: Laplace problem in mixed form

In this section we present the first application of the results shown in Section 4. The problem we want to solve is the same as in Section 5 (here $g=0$), but now we are using a mixed method to approximate it (see, for instance [11] for a review). Given two finite element space sequences $\Sigma_h \subset H(\operatorname{div};\Omega)$ and $V_h \subset L^2(\Omega)$, we look for $\boldsymbol{\sigma}_h \in \Sigma_h$ and $u_h \in V_h$ such that:

$$(\boldsymbol{\sigma}_h, \boldsymbol{\tau}) + (\operatorname{div}\boldsymbol{\tau}, u_h) = 0 \quad \forall \boldsymbol{\tau} \in \Sigma_h,$$
$$(\operatorname{div}\boldsymbol{\sigma}_h, v) = -(f, v) \qquad \forall v \in V_h.$$

The most popular choice of finite element spaces is to take Σ_h as the Raviart–Thomas space $\mathbf{RT}_k$ (see Section 4) and as V_h the space of discontinuous piecewise $\mathcal{Q}_k$ functions. Similarly to what we observed in Section 6 for Stokes problem, the space V_h can be defined in two different ways (local vs. global approach). Here the natural approach is the local one (the space is defined on the reference element and then mapped to the physical one), see [4].

Like in the previous sections of numerical examples, we consider a polynomial solution, so that the issues are not concerned with its regularity. We report the convergence results in Table 1. It is evident that Raviart–Thomas on distorted elements present poor approximation of the divergence, as it is forecasted by the theory of Section 4. On the other hand, the other components are well approximated even on distorted meshes. A proof of this results can be found in [4].

Table 2
Errors and orders of convergence for the mixed approximation to Poisson's equation

$\mathbf{ABF}_0$ on square meshes

n	$\|u-u_h\|_{L^2(\Omega)}$			$\|\boldsymbol{\sigma}-\boldsymbol{\sigma}_h\|_{L^2(\Omega)}$			$\|\operatorname{div}(\boldsymbol{\sigma}-\boldsymbol{\sigma}_h)\|_{L^2(\Omega)}$		
	err.	%	order	err.	%	order	err.	%	order
2	2.49e–02	74.59		6.89e–02	64.21		5.27e–02	7.54	
4	1.36e–02	40.65	0.9	3.42e–02	22.97	1.0	1.32e–02	1.88	2.0
8	7.03e–03	21.08	1.0	1.70e–02	11.43	1.0	3.29e–03	0.47	2.0
16	3.70e–03	11.10	0.9	8.51e–03	5.71	1.0	8.24e–04	0.12	2.0
32	1.93e–03	5.78	0.9	4.25e–03	2.85	1.0	2.06e–04	0.03	2.0

$\mathbf{ABF}_0$ on trapezoidal meshes

n	$\|u-u_h\|_{L^2(\Omega)}$			$\|\boldsymbol{\sigma}-\boldsymbol{\sigma}_h\|_{L^2(\Omega)}$			$\|\operatorname{div}(\boldsymbol{\sigma}-\boldsymbol{\sigma}_h)\|_{L^2(\Omega)}$		
	err.	%	order	err.	%	order	err.	%	order
2	2.31e–02	69.38		6.59e–02	44.20		6.91e–02	9.89	
4	1.33e–02	39.98	0.8	3.58e–02	24.04	0.9	3.58e–02	5.12	0.9
8	7.22e–03	21.66	0.9	1.85e–02	12.41	1.0	1.81e–02	2.58	1.0
16	3.84e–03	11.51	0.9	9.43e–03	6.33	1.0	9.05e–03	1.30	1.0
32	2.00e–03	5.99	0.9	4.77e–03	3.20	1.0	4.53e–03	0.65	1.0

Results where Σ_h is the new finite element space $\mathbf{ABF}_k$ and V_h is the space of mapped discontinuous piecewise polynomials of degree ad most $k+1$ are reported in Table 2. The optimal convergence is evident (on square meshes the divergence, as expected, is superconvergent).

8. Applications: acoustic eigenproblem and Maxwell eigenproblem

Our last example is the approximation of the eigenvalue problem: find $\lambda \in \mathbb{R}$ such that there exists a non vanishing vectorfield $\boldsymbol{\sigma} : \Omega \to \mathbb{R}^2$ which satisfies

$$\begin{aligned} &-\operatorname{grad}\operatorname{div}\boldsymbol{\sigma} = \lambda\boldsymbol{\sigma} && \text{in } \Omega,\\ &\operatorname{curl}\boldsymbol{\sigma} = 0 && \text{in } \Omega,\\ &\boldsymbol{\sigma}\cdot\mathbf{n} = 0 && \text{on } \partial\Omega, \end{aligned}$$

where $\mathbf{n}$ denotes the outward normal unit vector.

This eigenvalue problem has been studied in relation with problems arising from acoustics [18] or from fluid-structure interactions [5,16]. With a standard rotation of angle $\pi/2$ (mapping the divergence into the curl operator), it becomes the well-known curl Maxwell eigenvalue problem [9].

A standard way of dealing with this problem is to drop the curl free constraint (thus adding an infinite dimensional kernel to the operator) and to consider the approximate problem: given $\Sigma_h \subset H_0(\operatorname{div}; \Omega)$ (where the subscript refers to the vanishing boundary condition on the normal component), find $\lambda_h \in \mathbb{R}$ such that for a nonvanishing $\boldsymbol{\sigma}_h \in \Sigma_h$ it holds

$$(\operatorname{div}\boldsymbol{\sigma}_h, \operatorname{div}\boldsymbol{\tau}) = \lambda_h(\boldsymbol{\sigma}_h, \boldsymbol{\tau}) \quad \forall\boldsymbol{\tau} \in \Sigma_h.$$

It is well known (see, for instance, [6] for the case of three-dimensional Maxwell problem) that if Σ_h is chosen as the Raviart–Thomas space $\mathbf{RT}_k$ then eigenmodes corresponding to the nonvanishing eigenvalues of (8) are approximations of the eigenmodes of our original problem.

In Fig. 7 we report results of computations using the lowest order Raviart–Thomas elements $\mathbf{RT}_0$ where the results are stable, but there is no convergence (actually the discrete eigenvalues converge towards wrong numbers which depend on the mesh distortion). The meaning of the picture, is that each line represents the convergence history of one discrete eigenvalue. This bad behaviour has been observed also in [14]. There, an empirical explanation of this fact is proposed: an explicit computation shows that the ratio between the mass and stiffness matrices computed on the uniform and on the distorted mesh sequences, up to higher order terms, tends to one and to a number different from one, respectively.

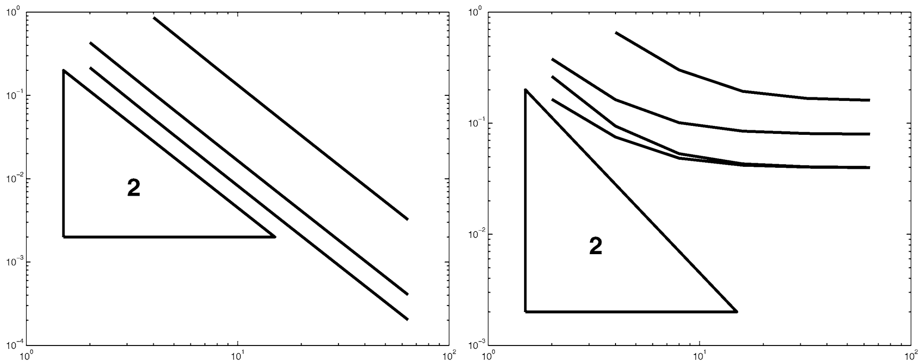

Fig. 7. Eigenvalue convergence on square (left) and trapezoidal (right) meshes for $\mathbf{RT}_0$ elements.

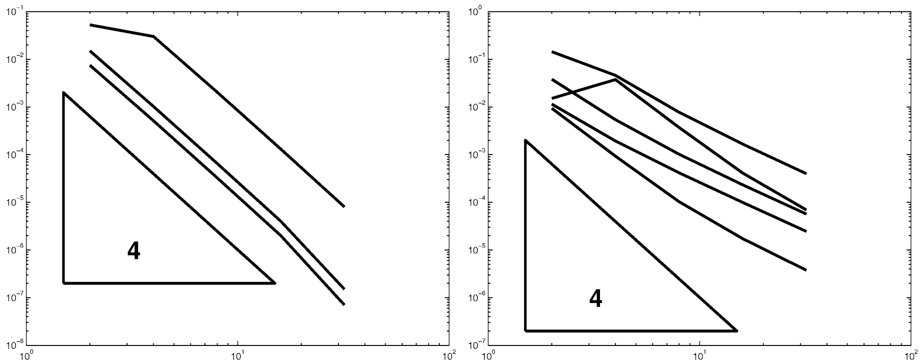

Fig. 8. Eigenvalue convergence on square (left) and trapezoidal (right) meshes for $\mathbf{RT}_1$ element.

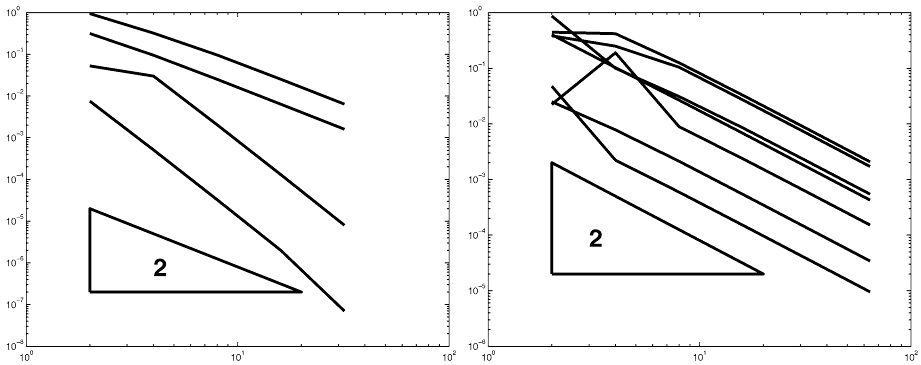

Fig. 9. Eigenvalue convergence on square (left) and trapezoidal (right) meshes for **ABF** elements.

On the other hand, in Fig. 9 we show the optimal convergence of the lowest order representative of our new family of finite elements $\mathbf{ABF}_0$. The good behavior of **ABF** element has been proved in [15] (we recall that good approximation properties are not enough for the correct approximation of the eigenmodes, see [10,8] for more details).

Our last computation shown in Fig. 8 is about the space $\mathbf{RT}_1$ where it is apparent that, on distorted meshes, the convergence properties deteriorate.

References

[1] D.N. Arnold, D. Boffi, R.S. Falk, L. Gastaldi, Finite element approximation on quadrilateral meshes, Comm. Numer. Methods Engrg. 17 (11) (2001) 805–812.
[2] D.N. Arnold, D. Boffi, R.S. Falk, Approximation by quadrilateral finite elements, Math. Comp. 71 (239) (2002) 909–922 (electronic).

[3] D.N. Arnold, D. Boffi, R.S. Falk, Remarks on quadrilateral Reissner–Mindlin plate elements, in: H.A. Mang, F.G. Rammerstorfer, J. Eberhardsteiner (Eds.), WCCM V, Fifth World Congress on Computational Mechanics, Vienna, Austria, July 7–12, 2002.
[4] D.N. Arnold, D. Boffi, R.S. Falk, Quadrilateral H(div) finite elements, SIAM J. Numer. Anal. 42 (2005) 2429–2451.
[5] A. Bermúdez, R. Durán, M.A. Muschietti, R. Rodríguez, J. Solomin, Finite element vibration analysis of fluid–solid systems without spurious modes, SIAM J. Numer. Anal. 32 (4) (1995) 1280–1295.
[6] D. Boffi, Fortin operator and discrete compactness for edge elements, Numer. Math. 87 (2) (2000) 229–246.
[7] D. Boffi, L. Gastaldi, On the quadrilateral Q_2–P_1 element for the Stokes problem, Internat. J. Numer. Methods Fluids 39 (11) (2002) 1001–1011.
[8] D. Boffi, F. Brezzi, L. Gastaldi, On the convergence of eigenvalues for mixed formulations, Ann. Scuola Norm. Sup. Pisa Cl. Sci. (4) 25 (1–2) (1997) 131–154 (1998) (dedicated to Ennio De Giorgi).
[9] D. Boffi, P. Fernandes, L. Gastaldi, I. Perugia, Computational models of electromagnetic resonators: Analysis of edge element approximation, SIAM J. Numer. Anal. 36 (4) (1999) 1264–1290 (electronic).
[10] D. Boffi, F. Brezzi, L. Gastaldi, On the problem of spurious eigenvalues in the approximation of linear elliptic problems in mixed form, Math. Comp. 69 (229) (2000) 121–140.
[11] F. Brezzi, M. Fortin, Mixed and Hybrid Finite Element Methods, Springer Series in Computational Mathematics, vol. 15, Springer, New York, 1991.
[12] P. Ciarlet, The Finite Element Method for Elliptic Problems, North-Holland, Amsterdam, 1978.
[13] P.G. Ciarlet, J.L. Lions (Eds.), Handbook of Numerical Analysis, vol. II, North-Holland, Amsterdam, 1991 (Finite element methods. Part 1).
[14] P. Gamallo, Contribución al estudio matemático de problemas de simulación elastoacústica y control activo del ruido, PhD thesis, Universidade de Santiago de Compostela, Spain, April 2002.
[15] F. Gardini, Discrete compactness property for quadrilateral finite element spaces, Numer. Methods Partial Differential Equations 21 (1) (2005) 41–56.
[16] L. Gastaldi, Mixed finite element methods in fluid structure systems, Numer. Math. 74 (2) (1996) 153–176.
[17] J. Thomas, Sur l'analyse numerique des methodes d'elements finis hybrides et mixes, PhD thesis, Université Pierre et Marie Curie, 1977.
[18] X. Wang, K.-J. Bathe, On mixed elements for acoustic fluid-structure interactions, Math. Models Methods Appl. Sci. 7 (3) (1997) 329–343.